*Macromolecules* 1992, *25*, 1941–1948

# CNDO Calculations for the Rotation of Aromatic Rings in Model Analogues of PEEK

**C. L. Chen,*,† J. L. Chang,† and A. C. Su*,‡**

*Department of Chemistry and Institute of Materials Science and Engineering, National Sun Yat-Sen University, Kaohsiung, Taiwan 80424, R.O.C.*

*Received September 6, 1991; Revised Manuscript Received December 10, 1991*

ABSTRACT: Rotational motions of the phenylene rings in PEEK were examined by means of semiempirical CNDO (complete neglect of differential overlap) molecular-orbital calculations for various model compounds. Results indicated that the ether–ether phenylene ring tends to stay coplanar with, whereas the ether–ketone ring prefers to lie vertical to, the plane of the backbone zigzag. This preferred arrangement results in low intramolecular hindrances for medium- to large-amplitude phenylene rotations or torsional motions of virtual bonds in amorphous PEEK. Upon crystallization, the phenylene rings give away their preferred angular positions and choose to incline by a low angle from the plane of the backbone zigzag in an alternating manner (as previous X-ray diffraction results dictate) to achieve efficient packing. The tight packing subsequently results in strong intermolecular interactions which, in combination with increased intramolecular hindrance (from stronger ring–ring repulsion at the low tilt angle), render motion of the phenylene rings restricted as observed in earlier solid-state NMR studies. Crankshaft types of chain motion are found consistent with the dielectrically determined activation energy for the $\gamma$-relaxation of PEEK.

## Introduction

Poly(oxy-1,4-phenyleneoxy-1,4-phenylenecarbonyl-1,4-phenylene), commonly known as PEEK, has become one of the major thermoplastic matrix materials for lightweight advanced composites.[1] The repeating unit of PEEK is shown in Figure 1. With a glass transition temperature ($T_g$) of ca. 140 °C, this polymer is semicrystalline and melts in the vicinity of 340 °C. Depending on the thermal history, the crystallinity may lie in the range of 0–50% but is often around 30% under typical processing conditions.[2-9] Results of previous X-ray diffraction studies[10-12] indicated that PEEK crystallizes into an orthorhombic structure with unit cell parameters $a = 0.78$ nm, $b = 0.59$ nm, and $c = 1.00$ nm. The unit cell contains two zigzagging chain strands, both are parallel to the $c$-axis, and each corresponds to two-thirds of a repeating unit; i.e., the ether–ether phenylene ring and the ether–ketone counterpart are crystallographically indistinguishable. These rings are inclined in an alternating manner to the plane to the backbone zigzag, the angle of inclination being ca. 40°. The angle between connecting virtual bonds is ca. 126°, higher than those expected for ether and carbonyl linkages.

In addition to its high continuous-service temperature (up to 200 °C)[13] attributable to the high melting temperature of the crystalline phase, PEEK bears good toughness. Fracture toughness or notched impact strength of extruded or molded specimens showed a clear dependence on processing conditions.[8,14,15] Sample characteristics such as crystallinity,[8,14] flow-induced orientation,[14] and spherulitic size[15] have been identified to bear significant effects on the mechanical properties of PEEK. On a different level, molecular motions in PEEK have also received increasing attention in recent years. A variety of techniques including dynamic mechanical spectroscopy,[16-18] dielectric spectroscopy,[18-19] and solid-state nuclear magnetic resonance spectroscopy (NMR)[20,21] have been used to explore molecular motions in PEEK.

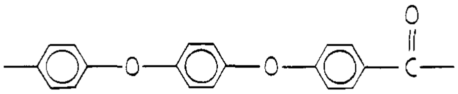

**Figure** 1. Structure of the repeating unit of PEEK.

The presence of a low-temperature loss peak (termed the $\gamma$-relaxation) near −70 °C in the dynamic mechanical spectrum of PEEK has been assigned to the local motion of phenylene rings by Sasuga and Hagiwara.[17] The activation energy of this secondary relaxation has been estimated to be 21 kcal/mol using dynamic mechanical spectroscopy in the frequency range $10^{-2}$–$10^2$ Hz; however, parallel dielectric measurements in the frequency range $10^2$–$10^5$ Hz indicated a much smaller value of ca. 10 kcal/mol for the activation energy.[18] Starkweather and Avakian[18] suggested that the dielectric loss peak is the high-frequency component of a broader distribution of motions revealed in the mechanical loss peak. In other words, the apparent activation energy determined via dynamic mechanical spectroscopy may represent the lumped temperature dependence for a range of molecular motions. The corresponding value determined by dielectric means is probably related to a fundamental molecular process presumably of a noncooperative nature.[18]

Clark et al.[20] studied amorphous and semicrystalline PEEK samples using both wide-line $^1$H NMR and cross-polarization magic angle spinning (CP/MAS) $^{13}$C NMR. The $^1$H lines of the semicrystalline sample (ca. 35% crystalline) were wider and exhibited longer spin–lattice relaxation times than those of the amorphous sample at temperatures below $T_g$. The temperature dependence of the proton spin–lattice relaxation time indicated an activation energy of 3.2 kcal/mol for both samples. The CP/MAS spectrum of the amorphous sample displayed broader signals than did the semicrystalline counterpart, suggesting a wider distribution of chemical shifts in the amorphous phase or the presence of molecular motion at frequencies comparable to the decoupling field. The optimum contact time was found shorter for the amorphous material. This was attributed to the faster spin–lattice relaxation of the protons in the amorphous sample. All these observations may be taken as indicative of higher segmental mobility of PEEK chains in the amorphous state.

A more recent CP/MAS $^{13}$C NMR study by Poliks and Schaefer[21] on two PEEK samples (ca. 1% and 26%

---

* To whom correspondence may be addressed.
† Department of Chemistry.
‡ Institute of Materials Science and Engineering.

0024-9297/92/2225-1941$03.00/0

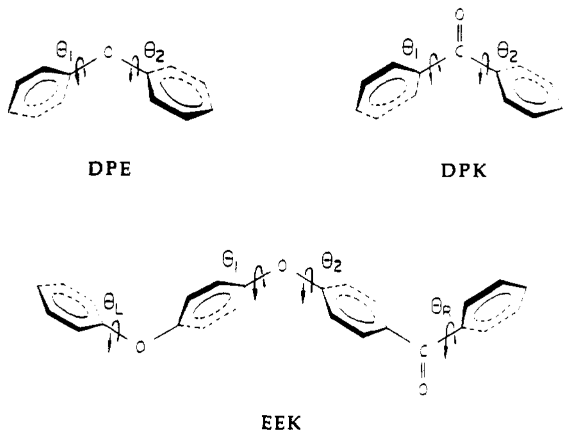

**Figure 2.** Structures of the model compounds for PEEK. The dihedral angle is defined as the angle between plane of the corresponding ring and the plane of the paper (molecular plane) in the direction indicated by the arrow.

crystalline, respectively) provided more specific conclusions on molecular motions in PEEK. Results of their dipolar rotational spin–echo experiments and observations on rotating-frame and laboratory spin–lattice relaxation times indicated that most of the phenylene rings in PEEK are immobile; only a limited fraction of phenylene rings in the amorphous phase are dynamically active. In the amorphous phase, the ether–ketone rings are slightly more mobile than the ether–ether rings. The average amplitude of ring rotation in the semicrystalline sample was qualitatively ranked less than that in Bisphenol A polycarbonate but higher than that in poly(ethylene terephthalate). This ranking is in interesting agreement with that according to typical values of notched Izod impact strength at room temperature. The more restricted nature of the ether–ether rings was attributed to the *inter*chain packing effects in the amorphous state.[21]

In addition to experimental efforts, theoretical calculations by use of molecular mechanics or quantum mechanical methods may serve to assist in the identification of the sources of *intra*chain interactions and the possible modes of molecular motion. Examples include our previous studies of polycarbonates.[22,23] In a recent work by Hay and Kemmish,[24] results of semiempirical self-consistent field calculations on various model compounds have been used to support the suggestion that *inter*chain packing interactions in the crystalline state may cause the observed alternative inclinations of phenylene rings along the PEEK chain as well as the variation in unit cell dimensions of PEEK with crystallization temperature.[25] Reported here are the results of our study for the rotation of phenylene in PEEK by use of the semiempirical CNDO/2 (complete neglect of differential overlap) method.[26] On the basis of the potential energy maps constructed, packing effects in the crystalline state, mobility of the aromatic rings, and possible mechanisms for the γ-relaxation in PEEK are discussed.

## Method of Calculation

Structures of the selected model compounds including diphenyl ether (DPE), benzophenone (or diphenyl ketone (DPK)), and phenyl phenyloxy-1,4-phenyleneoxy-1,4-phenylene ketone (EEK) are shown in Figure 2. The corresponding definitions of rotational angles are also given. The first two compounds are selected to observe the ring–ring interaction across an ether or a ketone linkage; the last is selected for the observation of interactions of a phenylene ring with its neighboring rings. The structure of EEK is such that both the ether–ether and the ether–ketone rings in PEEK are simulated. On the basis of the crystallographic information above and results of the semiempirical molecular orbital calculations by Hay and Kemmish,[24] bond angles and bond lengths in PEEK were assigned as those given in Table I.

**Table I**
**Structural Parameters Used in the CNDO Calculations**

| bond lengths, nm | | bond angles, deg | |
|---|---|---|---|
| C–C aromatic | 0.140 | C–C–C aromatic | 120 |
| C–H | 0.108 | H–C–C aromatic | 120 |
| C═O | 0.123 | C–C–C carbonyl | 126 |
| C–C nonaromatic | 0.142 | O–C–C carbonyl | 117 |
| C–O | 0.142 | C–O–C ether | 126 |

The CNDO/2 program of Pople[26] was used for the total energy calculation of DPE and DPK. In these calculations, the rotational angles of phenylene rings were varied in 10° increments whereas values of bond lengths and bond angles were assumed not to vary with the rotation of aromatic rings. Potential maps for the larger model compound EEK were calculated from those of DPE and DPK using the additive property[23,27] of the relative energies. For example, the unnormalized potential of EEK at $(\theta_1,\theta_2)$ may be estimated according to

$$E_{\mathrm{EKE}}(\theta_1,\theta_2) = E_{\mathrm{DPE}}(180°-\theta_1,180°-\theta_{\mathrm{L}}) + E_{\mathrm{DPE}}(\theta_1,\theta_2) + E_{\mathrm{DPK}}(180°-\theta_{\mathrm{R}},180°-\theta_2) \quad (1)$$

where $E$ represents the relative energy at the quoted angular position and subscripts DPE and DPK represent the respective model compounds. The relative energy map may be constructed after the identification of the absolute energy minimum. The feasibility of this approach has been verified using a series of model compounds.[27] Comparison between the energy map from direct CNDO calculations and the composite map generated from CNDO results of smaller model compounds (using equations similar to eq 1) indicated differences typically on the order of 0.1 kcal/mol, which may sometimes result in a slight shift (at most 10° in the present case of 10° increments in rotational angles) for the position of absolute energy minimum but affect little the general features of the potential map.

As discussed earlier,[23] the failure to allow adjustments in bond angles and bond lengths in the transition state would result in an overestimation for the potential barrier of interest. On the other hand, a polymer chain in the condensed state is surrounded by relatively immobile neighboring entities. The presence of surrounding molecular entities along a chain exerts resistance to the structural adjustment of a specific segment (i.e., the "model compound") in its transition state. This matrix effect[28,29] draws more or less the specific segment back to structural rigidity. In other words, the simplifying assumption of structural rigidity may actually bring the model compounds closer to the situation of real chain segments in the condensed state as compared to the case of a solitary molecule in a vacuum. This appears especially applicable in the case of polymers of long virtual bonds (such as the present case of PEEK) due to increased intermolecular interactions.

In two separate molecular mechanics studies of poly(methyl methacrylate) (PMMA) and related polymers, Cowie and Ferguson[28] and Heijboer et al.[29] independently noted that the calculated barrier to rotation of the alkoxycarbonyl group (which they considered responsible for the β-relaxation of PMMA) was much too low if structural optimization was allowed. If, on the other hand, the

| $\theta_1$ \ $\theta_2$ | | | | | | | | | 90° | | | | | | | | | 180° | | | | | | | | | 270° | | | | | | | | | 360° |
|---|---|---|---|---|---|---|---|---|---|---|---|---|---|---|---|---|---|---|---|---|---|---|---|---|---|---|---|---|---|---|---|---|---|---|---|---|
| | 21 | 7 | 1 | 0 | 0 | 0 | 1 | 1 | 1 | 1 | 1 | 0 | 1 | 4 | 14 | 35 | 54 | 44 | 21 | 7 | 1 | 0 | 0 | 0 | 1 | 1 | 1 | 1 | 1 | 0 | 1 | 4 | 14 | 35 | 54 | 44 |
| | 7 | 2 | 0 | 0 | 0 | 1 | 1 | 1 | 1 | 1 | 1 | 1 | 3 | 9 | 23 | 38 | 35 | 19 | 7 | 2 | 0 | 0 | 0 | 1 | 1 | 1 | 1 | 1 | 1 | 1 | 3 | 9 | 23 | 38 | 35 | 19 |
| | 1 | 0 | ● | 0 | 1 | 1 | 1 | 1 | 1 | 1 | 1 | 2 | 5 | 12 | 21 | 23 | 14 | 6 | 1 | 0 | ● | 0 | 1 | 1 | 1 | 1 | 1 | 1 | 1 | 2 | 5 | 12 | 21 | 23 | 14 | 6 |
| | 0 | 0 | 0 | 1 | 1 | 1 | 2 | 2 | 2 | 2 | 2 | 3 | 6 | 10 | 12 | 9 | 4 | 1 | 0 | 0 | 0 | 1 | 1 | 1 | 2 | 2 | 2 | 2 | 2 | 3 | 6 | 10 | 12 | 9 | 4 | 1 |
| | 0 | 0 | 1 | 1 | 1 | 2 | 2 | 2 | 2 | 2 | 2 | 3 | 5 | 6 | 5 | 3 | 1 | 0 | 0 | 0 | 1 | 1 | 1 | 2 | 2 | 2 | 2 | 2 | 2 | 3 | 5 | 6 | 5 | 3 | 1 | 0 |
| | 0 | 1 | 1 | 1 | 2 | 2 | 2 | 2 | 2 | 2 | 2 | 3 | 3 | 3 | 2 | 1 | 0 | 0 | 0 | 1 | 1 | 1 | 2 | 2 | 2 | 2 | 2 | 2 | 2 | 3 | 3 | 3 | 2 | 1 | 0 | 0 |
| | 1 | 1 | 1 | 2 | 2 | 2 | 2 | 2 | 2 | 2 | 2 | 2 | 2 | 2 | 1 | 1 | 1 | 1 | 1 | 1 | 1 | 2 | 2 | 2 | 2 | 2 | 2 | 2 | 2 | 2 | 2 | 2 | 1 | 1 | 1 | 1 |
| | 1 | 1 | 1 | 2 | 2 | 2 | 2 | 3 | 3 | 3 | 2 | 2 | 2 | 2 | 1 | 1 | 1 | 1 | 1 | 1 | 1 | 2 | 2 | 2 | 2 | 3 | 3 | 3 | 2 | 2 | 2 | 2 | 1 | 1 | 1 | 1 |
| 90° | 1 | 1 | 1 | 2 | 2 | 2 | 2 | 3 | 3 | 3 | 2 | 2 | 2 | 2 | 1 | 1 | 1 | 1 | 1 | 1 | 1 | 2 | 2 | 2 | 2 | 3 | 3 | 3 | 2 | 2 | 2 | 2 | 1 | 1 | 1 | 1 |
| | 1 | 1 | 1 | 2 | 2 | 2 | 2 | 3 | 3 | 3 | 2 | 2 | 2 | 2 | 1 | 1 | 1 | 1 | 1 | 1 | 1 | 2 | 2 | 2 | 2 | 3 | 3 | 3 | 2 | 2 | 2 | 2 | 1 | 1 | 1 | 1 |
| | 1 | 1 | 1 | 2 | 2 | 2 | 2 | 2 | 2 | 2 | 2 | 2 | 2 | 2 | 1 | 1 | 1 | 1 | 1 | 1 | 1 | 2 | 2 | 2 | 2 | 2 | 2 | 2 | 2 | 2 | 2 | 2 | 1 | 1 | 1 | 1 |
| | 0 | 1 | 2 | 3 | 3 | 3 | 2 | 2 | 2 | 2 | 2 | 2 | 2 | 1 | 1 | 1 | 0 | 0 | 0 | 1 | 2 | 3 | 3 | 3 | 2 | 2 | 2 | 2 | 2 | 2 | 2 | 1 | 1 | 1 | 0 | 0 |
| | 1 | 3 | 5 | 6 | 5 | 3 | 2 | 2 | 2 | 2 | 2 | 2 | 1 | 1 | 1 | 0 | 0 | 0 | 1 | 3 | 5 | 6 | 5 | 3 | 2 | 2 | 2 | 2 | 2 | 2 | 1 | 1 | 1 | 0 | 0 | 0 |
| | 4 | 9 | 12 | 10 | 6 | 3 | 2 | 2 | 2 | 2 | 2 | 1 | 1 | 1 | 0 | 0 | 0 | 1 | 4 | 9 | 12 | 10 | 6 | 3 | 2 | 2 | 2 | 2 | 2 | 1 | 1 | 1 | 0 | 0 | 0 | 1 |
| | 14 | 23 | 21 | 12 | 5 | 2 | 1 | 1 | 1 | 1 | 1 | 1 | 1 | 0 | 0 | 0 | 0 | 6 | 14 | 23 | 21 | 12 | 5 | 2 | 1 | 1 | 1 | 1 | 1 | 1 | 1 | 0 | 0 | 0 | 0 | 6 |
| | 35 | 38 | 23 | 9 | 3 | 1 | 1 | 1 | 1 | 1 | 1 | 1 | 0 | 0 | 0 | 2 | 7 | 19 | 35 | 38 | 23 | 9 | 3 | 1 | 1 | 1 | 1 | 1 | 1 | 1 | 0 | 0 | 0 | 2 | 7 | 19 |
| | 54 | 35 | 14 | 4 | 1 | 0 | 1 | 1 | 1 | 1 | 1 | 0 | 0 | 0 | 1 | 7 | 21 | 44 | 54 | 35 | 14 | 4 | 1 | 0 | 1 | 1 | 1 | 1 | 1 | 0 | 0 | 0 | 1 | 7 | 21 | 44 |
| 180° | 44 | 19 | 6 | 1 | 0 | 0 | 1 | 1 | 1 | 1 | 1 | 0 | 0 | 1 | 6 | 19 | 44 | 61 | 44 | 19 | 6 | 1 | 0 | 0 | 1 | 1 | 1 | 1 | 1 | 0 | 0 | 1 | 6 | 19 | 44 | 61 |
| | 21 | 7 | 1 | 0 | 0 | 0 | 1 | 1 | 1 | 1 | 1 | 0 | 1 | 4 | 14 | 35 | 54 | 44 | 21 | 7 | 1 | 0 | 0 | 0 | 1 | 1 | 1 | 1 | 1 | 0 | 1 | 4 | 14 | 35 | 54 | 44 |
| | 7 | 2 | 0 | 0 | 0 | 1 | 1 | 1 | 1 | 1 | 1 | 1 | 3 | 9 | 23 | 38 | 35 | 19 | 7 | 2 | 0 | 0 | 0 | 1 | 1 | 1 | 1 | 1 | 1 | 1 | 3 | 9 | 23 | 38 | 35 | 19 |
| | 1 | 0 | ● | 0 | 1 | 1 | 1 | 1 | 1 | 1 | 1 | 2 | 5 | 12 | 21 | 23 | 14 | 6 | 1 | 0 | ● | 0 | 1 | 1 | 1 | 1 | 1 | 1 | 1 | 2 | 5 | 12 | 21 | 23 | 14 | 6 |
| | 0 | 0 | 0 | 1 | 1 | 1 | 2 | 2 | 2 | 2 | 2 | 3 | 6 | 10 | 12 | 9 | 4 | 1 | 0 | 0 | 0 | 1 | 1 | 1 | 2 | 2 | 2 | 2 | 2 | 3 | 6 | 10 | 12 | 9 | 4 | 1 |
| | 0 | 0 | 1 | 1 | 1 | 2 | 2 | 2 | 2 | 2 | 2 | 3 | 5 | 6 | 5 | 3 | 1 | 0 | 0 | 0 | 1 | 1 | 1 | 2 | 2 | 2 | 2 | 2 | 2 | 3 | 5 | 6 | 5 | 3 | 1 | 0 |
| | 0 | 1 | 1 | 1 | 2 | 2 | 2 | 2 | 2 | 2 | 2 | 3 | 3 | 3 | 2 | 1 | 0 | 0 | 0 | 1 | 1 | 1 | 2 | 2 | 2 | 2 | 2 | 2 | 2 | 3 | 3 | 3 | 2 | 1 | 0 | 0 |
| | 1 | 1 | 1 | 2 | 2 | 2 | 2 | 2 | 2 | 2 | 2 | 2 | 2 | 2 | 1 | 1 | 1 | 1 | 1 | 1 | 1 | 2 | 2 | 2 | 2 | 2 | 2 | 2 | 2 | 2 | 2 | 2 | 1 | 1 | 1 | 1 |
| | 1 | 1 | 1 | 2 | 2 | 2 | 2 | 3 | 3 | 3 | 2 | 2 | 2 | 2 | 1 | 1 | 1 | 1 | 1 | 1 | 1 | 2 | 2 | 2 | 2 | 3 | 3 | 3 | 2 | 2 | 2 | 2 | 1 | 1 | 1 | 1 |
| 270° | 1 | 1 | 1 | 2 | 2 | 2 | 2 | 3 | 3 | 3 | 2 | 2 | 2 | 2 | 1 | 1 | 1 | 1 | 1 | 1 | 1 | 2 | 2 | 2 | 2 | 3 | 3 | 3 | 2 | 2 | 2 | 2 | 1 | 1 | 1 | 1 |
| | 1 | 1 | 1 | 2 | 2 | 2 | 2 | 3 | 3 | 3 | 2 | 2 | 2 | 2 | 1 | 1 | 1 | 1 | 1 | 1 | 1 | 2 | 2 | 2 | 2 | 3 | 3 | 3 | 2 | 2 | 2 | 2 | 1 | 1 | 1 | 1 |
| | 1 | 1 | 1 | 2 | 2 | 2 | 2 | 2 | 2 | 2 | 2 | 2 | 2 | 2 | 1 | 1 | 1 | 1 | 1 | 1 | 1 | 2 | 2 | 2 | 2 | 2 | 2 | 2 | 2 | 2 | 2 | 2 | 1 | 1 | 1 | 1 |
| | 0 | 1 | 2 | 3 | 3 | 3 | 2 | 2 | 2 | 2 | 2 | 2 | 2 | 1 | 1 | 1 | 0 | 0 | 0 | 1 | 2 | 3 | 3 | 3 | 2 | 2 | 2 | 2 | 2 | 2 | 2 | 1 | 1 | 1 | 0 | 0 |
| | 1 | 3 | 5 | 6 | 5 | 3 | 2 | 2 | 2 | 2 | 2 | 2 | 1 | 1 | 1 | 0 | 0 | 0 | 1 | 3 | 5 | 6 | 5 | 3 | 2 | 2 | 2 | 2 | 2 | 2 | 1 | 1 | 1 | 0 | 0 | 0 |
| | 4 | 9 | 12 | 10 | 6 | 3 | 2 | 2 | 2 | 2 | 2 | 1 | 1 | 1 | 0 | 0 | 0 | 1 | 4 | 9 | 12 | 10 | 6 | 3 | 2 | 2 | 2 | 2 | 2 | 1 | 1 | 1 | 0 | 0 | 0 | 1 |
| | 14 | 23 | 21 | 12 | 5 | 2 | 1 | 1 | 1 | 1 | 1 | 1 | 1 | 0 | 0 | 0 | 0 | 6 | 14 | 23 | 21 | 12 | 5 | 2 | 1 | 1 | 1 | 1 | 1 | 1 | 1 | 0 | 0 | 0 | 0 | 6 |
| | 35 | 38 | 23 | 9 | 3 | 1 | 1 | 1 | 1 | 1 | 1 | 1 | 0 | 0 | 0 | 2 | 7 | 19 | 35 | 38 | 23 | 9 | 3 | 1 | 1 | 1 | 1 | 1 | 1 | 1 | 0 | 0 | 0 | 2 | 7 | 19 |
| | 54 | 35 | 14 | 4 | 1 | 0 | 1 | 1 | 1 | 1 | 1 | 0 | 0 | 0 | 1 | 7 | 21 | 44 | 54 | 35 | 14 | 4 | 1 | 0 | 1 | 1 | 1 | 1 | 1 | 0 | 0 | 0 | 1 | 7 | 21 | 44 |
| 360° | 44 | 19 | 6 | 1 | 0 | 0 | 1 | 1 | 1 | 1 | 1 | 0 | 0 | 1 | 6 | 19 | 44 | 61 | 44 | 19 | 6 | 1 | 0 | 0 | 1 | 1 | 1 | 1 | 1 | 0 | 0 | 1 | 6 | 19 | 44 | 61 |

**Figure 3.** Relative conformation energies (in kcal/mol) for the rotation of the phenyl rings in DPE. The filled circles (●) indicate absolute energy minima. Values in the potential map have been rounded into integers.

movements of the main chain and neighboring groups were assumed constrained, the calculated barrier was brought near the experiment activation energy of the $\beta$-process. It was concluded that approximately half of the experimental barrier may be attributed to the matrix effect. This is in interesting agreement with an earlier analysis of Yannas and Luise,[30] who suggested that deformation of glassy polymers involves important contributions from the "intermolecular barrier". For polymers of short virtual bonds such as PMMA, they estimated that the "intermolecular barrier" contribution may equal the "intramolecular barrier" contribution. For polymers of long virtual bonds such as Bisphenol A polycarbonate (PC), they concluded that the "intermolecular barrier" dominates. In our previous CNDO studies[22,23] of PC where the assumption of structural rigidity was adopted, the agreement between the calculated rotational barrier of ca. 12 kcal/mol and the experimental values of 9–12 kcal/mol (determined from solid-state NMR measurements[31,32]) for 180° ring flips in PC has been interpreted as a direct consequence of the strong matrix effect involved.

In spite of the justifying arguments above, the fact remains that our simplifying assumptions do introduce some uncertainties. Results of the present study should therefore be considered semiquantitative at best.

## Results and Discussion

**DPE.** Given in Figure 3 is the potential map of DPE. The absolute minima are at $(\theta_1,\theta_2) = (30°,30°)$ or the equivalent, in reasonable agreement with the experimentally observed alternative inclination angle of ca. 40° from the plane of the zigzagging PEEK backbone. The aromatic rings resist coplanarity (where the absolute energy maximum appears), similar to the previously studied case of diphenylisopropylidene.[22] This may be attributable to the repulsion between ortho hydrogens on different rings. Interestingly, there exist local potential maxima at $(\theta_1,\theta_2) = (90°,90°)$ or the equivalent, with a relative energy slightly less than 3 kcal/mol. These angular positions represent the case of lowest core–core repulsion between ortho hydrogens. The only moderate tilt of aromatic rings from the molecular plane at their equilibrium positions and the presence of local potential maxima at $(\theta_1,\theta_2) = (90°,90°)$ or the equivalent indicate significant contributions from electron delocalization.

Two possible types of large-amplitude ring motion can be identified. The first is the 180° flip of one ring while the other ring remains at its equilibrium position. The corresponding activation energy is relatively high (ca. 23 kcal/mol), due mainly to the repulsion between ortho hydrogens.[22] The second type of ring motion is the synchronous rotation of the two rings. In this case, the distance between ortho hydrogens on separate rings remains constant, resulting in a low energy barrier of ca. 2 kcal/mol. For reasons to be apparent later, if the rings can be located at $(\theta_1,\theta_2) = (0°,90°)$ or the equivalent, there exists another type of 180° flip in which the "horizontal" ring flips while the "vertical" ring remains fixed. The barrier to this additional type of ring flip is only ca. 2 kcal/mol, due to minimized repulsion between ortho hydrogens.

**DPK.** Given in Figure 4 is the potential map of DPK. The absolute minima correspond to $(\theta_1,\theta_2) = (90°,90°)$ or the equivalent, quite different from the reported inclination angle of 40° in crystalline PEEK. The tendency for the two rings to avoid the coplanar conformation is

| $\theta_1$ \ $\theta_2$ |  |  |  |  |  |  |  |  | 90° |  |  |  |  |  |  |  |  | 180° |  |  |  |  |  |  |  |  | 270° |  |  |  |  |  |  |  |  | 360° |
|---|---|---|---|---|---|---|---|---|---|---|---|---|---|---|---|---|---|---|---|---|---|---|---|---|---|---|---|---|---|---|---|---|---|---|---|---|
|  | 25 | 11 | 5 | 3 | 3 | 2 | 2 | 2 | 2 | 2 | 2 | 2 | 3 | 7 | 18 | 39 | 59 | 49 | 25 | 11 | 5 | 3 | 3 | 2 | 2 | 2 | 2 | 2 | 2 | 2 | 3 | 7 | 18 | 39 | 59 | 49 |
|  | 11 | 5 | 3 | 3 | 2 | 2 | 2 | 2 | 2 | 2 | 2 | 2 | 5 | 11 | 26 | 42 | 39 | 23 | 11 | 5 | 3 | 3 | 2 | 2 | 2 | 2 | 2 | 2 | 2 | 2 | 5 | 11 | 26 | 42 | 39 | 23 |
|  | 5 | 3 | 3 | 2 | 2 | 2 | 2 | 2 | 1 | 1 | 2 | 3 | 6 | 14 | 24 | 26 | 18 | 9 | 5 | 3 | 3 | 2 | 2 | 2 | 2 | 2 | 1 | 1 | 2 | 3 | 6 | 14 | 24 | 26 | 18 | 9 |
|  | 3 | 3 | 2 | 2 | 2 | 2 | 1 | 1 | 1 | 1 | 1 | 3 | 6 | 11 | 14 | 11 | 7 | 4 | 3 | 3 | 2 | 2 | 2 | 2 | 1 | 1 | 1 | 1 | 1 | 3 | 6 | 11 | 14 | 11 | 7 | 4 |
|  | 3 | 2 | 2 | 2 | 2 | 1 | 1 | 1 | 1 | 1 | 1 | 2 | 4 | 6 | 6 | 5 | 3 | 3 | 3 | 2 | 2 | 2 | 2 | 1 | 1 | 1 | 1 | 1 | 1 | 2 | 4 | 6 | 6 | 5 | 3 | 3 |
|  | 2 | 2 | 2 | 2 | 1 | 1 | 1 | 1 | 0 | 0 | 1 | 2 | 2 | 3 | 3 | 2 | 2 | 2 | 2 | 2 | 2 | 2 | 1 | 1 | 1 | 1 | 0 | 0 | 1 | 2 | 2 | 3 | 3 | 2 | 2 | 2 |
|  | 2 | 2 | 2 | 1 | 1 | 1 | 0 | 0 | 0 | 0 | 0 | 1 | 1 | 1 | 2 | 2 | 2 | 2 | 2 | 2 | 2 | 1 | 1 | 1 | 0 | 0 | 0 | 0 | 0 | 1 | 1 | 1 | 2 | 2 | 2 | 2 |
|  | 2 | 2 | 2 | 1 | 1 | 1 | 0 | 0 | 0 | 0 | 0 | 0 | 1 | 1 | 1 | 2 | 2 | 2 | 2 | 2 | 2 | 1 | 1 | 1 | 0 | 0 | 0 | 0 | 0 | 0 | 1 | 1 | 1 | 2 | 2 | 2 |
| 90° | 2 | 2 | 1 | 1 | 1 | 0 | 0 | 0 | ● | 0 | 0 | 0 | 1 | 1 | 1 | 2 | 2 | 2 | 2 | 2 | 1 | 1 | 1 | 0 | 0 | 0 | ● | 0 | 0 | 0 | 1 | 1 | 1 | 2 | 2 | 2 |
|  | 2 | 2 | 1 | 1 | 1 | 0 | 0 | 0 | 0 | 0 | 0 | 1 | 1 | 1 | 2 | 2 | 2 | 2 | 2 | 2 | 1 | 1 | 1 | 0 | 0 | 0 | 0 | 0 | 0 | 1 | 1 | 1 | 2 | 2 | 2 | 2 |
|  | 2 | 2 | 2 | 1 | 1 | 1 | 0 | 0 | 0 | 0 | 0 | 1 | 1 | 1 | 2 | 2 | 2 | 2 | 2 | 2 | 2 | 1 | 1 | 1 | 0 | 0 | 0 | 0 | 0 | 1 | 1 | 1 | 2 | 2 | 2 | 2 |
|  | 2 | 2 | 3 | 3 | 2 | 2 | 1 | 0 | 0 | 1 | 1 | 1 | 1 | 2 | 2 | 2 | 2 | 2 | 2 | 2 | 3 | 3 | 2 | 2 | 1 | 0 | 0 | 1 | 1 | 1 | 1 | 2 | 2 | 2 | 2 | 2 |
|  | 3 | 5 | 6 | 6 | 4 | 2 | 1 | 1 | 1 | 1 | 1 | 1 | 2 | 2 | 2 | 2 | 3 | 3 | 3 | 5 | 6 | 6 | 4 | 2 | 1 | 1 | 1 | 1 | 1 | 1 | 2 | 2 | 2 | 2 | 3 | 3 |
|  | 7 | 11 | 14 | 11 | 6 | 3 | 1 | 1 | 1 | 1 | 1 | 2 | 2 | 2 | 2 | 3 | 3 | 4 | 7 | 11 | 14 | 11 | 6 | 3 | 1 | 1 | 1 | 1 | 1 | 2 | 2 | 2 | 2 | 3 | 3 | 4 |
|  | 18 | 26 | 24 | 14 | 6 | 3 | 2 | 1 | 1 | 2 | 2 | 2 | 2 | 2 | 3 | 3 | 5 | 9 | 18 | 26 | 24 | 14 | 6 | 3 | 2 | 1 | 1 | 2 | 2 | 2 | 2 | 2 | 3 | 3 | 5 | 9 |
|  | 39 | 42 | 26 | 11 | 5 | 2 | 2 | 2 | 2 | 2 | 2 | 2 | 2 | 3 | 3 | 5 | 11 | 23 | 39 | 42 | 26 | 11 | 5 | 2 | 2 | 2 | 2 | 2 | 2 | 2 | 2 | 3 | 3 | 5 | 11 | 23 |
|  | 59 | 39 | 18 | 7 | 3 | 2 | 2 | 2 | 2 | 2 | 2 | 2 | 3 | 3 | 5 | 11 | 25 | 49 | 59 | 39 | 18 | 7 | 3 | 2 | 2 | 2 | 2 | 2 | 2 | 2 | 3 | 3 | 5 | 11 | 25 | 49 |
| 180° | 49 | 23 | 9 | 4 | 3 | 2 | 2 | 2 | 2 | 2 | 2 | 2 | 3 | 4 | 9 | 23 | 49 | 67 | 49 | 23 | 9 | 4 | 3 | 2 | 2 | 2 | 2 | 2 | 2 | 2 | 3 | 4 | 9 | 23 | 49 | 67 |
|  | 25 | 11 | 5 | 3 | 3 | 2 | 2 | 2 | 2 | 2 | 2 | 2 | 3 | 7 | 18 | 39 | 59 | 49 | 25 | 11 | 5 | 3 | 3 | 2 | 2 | 2 | 2 | 2 | 2 | 2 | 3 | 7 | 18 | 39 | 59 | 49 |
|  | 11 | 5 | 3 | 3 | 2 | 2 | 2 | 2 | 2 | 2 | 2 | 2 | 5 | 11 | 26 | 42 | 39 | 23 | 11 | 5 | 3 | 3 | 2 | 2 | 2 | 2 | 2 | 2 | 2 | 2 | 5 | 11 | 26 | 42 | 39 | 23 |
|  | 5 | 3 | 3 | 2 | 2 | 2 | 2 | 2 | 1 | 1 | 2 | 3 | 6 | 14 | 24 | 26 | 18 | 9 | 5 | 3 | 3 | 2 | 2 | 2 | 2 | 2 | 1 | 1 | 2 | 3 | 6 | 14 | 24 | 26 | 18 | 9 |
|  | 3 | 3 | 2 | 2 | 2 | 2 | 1 | 1 | 1 | 1 | 1 | 3 | 6 | 11 | 14 | 11 | 7 | 4 | 3 | 3 | 2 | 2 | 2 | 2 | 1 | 1 | 1 | 1 | 1 | 3 | 6 | 11 | 14 | 11 | 7 | 4 |
|  | 3 | 2 | 2 | 2 | 2 | 1 | 1 | 1 | 1 | 1 | 1 | 2 | 4 | 6 | 6 | 5 | 3 | 3 | 3 | 2 | 2 | 2 | 2 | 1 | 1 | 1 | 1 | 1 | 1 | 2 | 4 | 6 | 6 | 5 | 3 | 3 |
|  | 2 | 2 | 2 | 2 | 1 | 1 | 1 | 1 | 0 | 0 | 1 | 2 | 2 | 3 | 3 | 2 | 2 | 2 | 2 | 2 | 2 | 2 | 1 | 1 | 1 | 1 | 0 | 0 | 1 | 2 | 2 | 3 | 3 | 2 | 2 | 2 |
|  | 2 | 2 | 2 | 1 | 1 | 1 | 0 | 0 | 0 | 0 | 0 | 1 | 1 | 1 | 2 | 2 | 2 | 2 | 2 | 2 | 2 | 1 | 1 | 1 | 0 | 0 | 0 | 0 | 0 | 1 | 1 | 1 | 2 | 2 | 2 | 2 |
|  | 2 | 2 | 2 | 1 | 1 | 1 | 0 | 0 | 0 | 0 | 0 | 0 | 1 | 1 | 1 | 2 | 2 | 2 | 2 | 2 | 2 | 1 | 1 | 1 | 0 | 0 | 0 | 0 | 0 | 0 | 1 | 1 | 1 | 2 | 2 | 2 |
| 270° | 2 | 2 | 1 | 1 | 1 | 0 | 0 | 0 | ● | 0 | 0 | 0 | 1 | 1 | 1 | 2 | 2 | 2 | 2 | 2 | 1 | 1 | 1 | 0 | 0 | 0 | ● | 0 | 0 | 0 | 1 | 1 | 1 | 2 | 2 | 2 |
|  | 2 | 2 | 1 | 1 | 1 | 0 | 0 | 0 | 0 | 0 | 0 | 1 | 1 | 1 | 2 | 2 | 2 | 2 | 2 | 2 | 1 | 1 | 1 | 0 | 0 | 0 | 0 | 0 | 0 | 1 | 1 | 1 | 2 | 2 | 2 | 2 |
|  | 2 | 2 | 2 | 1 | 1 | 1 | 0 | 0 | 0 | 0 | 0 | 1 | 1 | 1 | 2 | 2 | 2 | 2 | 2 | 2 | 2 | 1 | 1 | 1 | 0 | 0 | 0 | 0 | 0 | 1 | 1 | 1 | 2 | 2 | 2 | 2 |
|  | 2 | 2 | 3 | 3 | 2 | 2 | 1 | 0 | 0 | 1 | 1 | 1 | 1 | 2 | 2 | 2 | 2 | 2 | 2 | 2 | 3 | 3 | 2 | 2 | 1 | 0 | 0 | 1 | 1 | 1 | 1 | 2 | 2 | 2 | 2 | 2 |
|  | 3 | 5 | 6 | 6 | 4 | 2 | 1 | 1 | 1 | 1 | 1 | 1 | 2 | 2 | 2 | 2 | 3 | 3 | 3 | 5 | 6 | 6 | 4 | 2 | 1 | 1 | 1 | 1 | 1 | 1 | 2 | 2 | 2 | 2 | 3 | 3 |
|  | 7 | 11 | 14 | 11 | 6 | 3 | 1 | 1 | 1 | 1 | 1 | 2 | 2 | 2 | 2 | 3 | 3 | 4 | 7 | 11 | 14 | 11 | 6 | 3 | 1 | 1 | 1 | 1 | 1 | 2 | 2 | 2 | 2 | 3 | 3 | 4 |
|  | 18 | 26 | 24 | 14 | 6 | 3 | 2 | 1 | 1 | 2 | 2 | 2 | 2 | 2 | 3 | 3 | 5 | 9 | 18 | 26 | 24 | 14 | 6 | 3 | 2 | 1 | 1 | 2 | 2 | 2 | 2 | 2 | 3 | 3 | 5 | 9 |
|  | 39 | 42 | 26 | 11 | 5 | 2 | 2 | 2 | 2 | 2 | 2 | 2 | 2 | 3 | 3 | 5 | 11 | 23 | 39 | 42 | 26 | 11 | 5 | 2 | 2 | 2 | 2 | 2 | 2 | 2 | 2 | 3 | 3 | 5 | 11 | 23 |
|  | 59 | 39 | 18 | 7 | 3 | 2 | 2 | 2 | 2 | 2 | 2 | 2 | 3 | 3 | 5 | 11 | 25 | 49 | 59 | 39 | 18 | 7 | 3 | 2 | 2 | 2 | 2 | 2 | 2 | 2 | 3 | 3 | 5 | 11 | 25 | 49 |
| 360° | 49 | 23 | 9 | 4 | 3 | 2 | 2 | 2 | 2 | 2 | 2 | 2 | 3 | 4 | 9 | 23 | 49 | 67 | 49 | 23 | 9 | 4 | 3 | 2 | 2 | 2 | 2 | 2 | 2 | 2 | 3 | 4 | 9 | 23 | 49 | 67 |

**Figure 4.** Relative conformation energies (in kcal/mol) for the rotation of the phenyl rings in DPK. The filled circles (●) indicate absolute energy minima. Values in the potential map have been rounded into integers.

| $\theta_{ee}$ \ $\theta_{ek}$ |  |  |  |  |  | 60° |  |  |  |  |  | 120° |  |  |  |  |  | 180° |
|---|---|---|---|---|---|---|---|---|---|---|---|---|---|---|---|---|---|---|
|  | 65 | 17 | 4 | 1 | 0 | 0 | 0 | 0 | 0 | 0 | 0 | 0 | 2 | 9 | 29 | 73 | XX | XX |
|  | 37 | 7 | 2 | 1 | 1 | 1 | 1 | 1 | 1 | 1 | 1 | 2 | 6 | 18 | 46 | 79 | 94 | XX |
|  | 27 | 4 | 1 | 1 | 1 | 1 | 1 | 1 | 1 | 1 | 1 | 3 | 10 | 25 | 43 | 49 | 52 | 75 |
|  | 24 | 4 | 2 | 2 | 2 | 2 | 2 | 2 | 2 | 2 | 3 | 5 | 11 | 21 | 25 | 21 | 32 | 66 |
|  | 24 | 4 | 3 | 3 | 3 | 3 | 3 | 3 | 3 | 3 | 3 | 6 | 9 | 12 | 11 | 9 | 26 | 64 |
| 60° | 25 | 5 | 3 | 3 | 3 | 3 | 3 | 3 | 3 | 3 | 4 | 5 | 6 | 6 | 5 | 6 | 25 | 64 |
|  | 25 | 5 | 3 | 4 | 4 | 4 | 4 | 4 | 4 | 4 | 4 | 4 | 5 | 4 | 4 | 5 | 25 | 64 |
|  | 25 | 5 | 4 | 4 | 4 | 4 | 4 | 4 | 4 | 4 | 4 | 4 | 4 | 4 | 4 | 5 | 25 | 64 |
|  | 25 | 6 | 4 | 4 | 4 | 4 | 4 | 4 | 4 | 4 | 4 | 4 | 4 | 4 | 4 | 5 | 25 | 64 |
|  | 25 | 5 | 4 | 4 | 4 | 4 | 4 | 4 | 4 | 4 | 4 | 4 | 4 | 4 | 4 | 5 | 25 | 64 |
|  | 25 | 5 | 4 | 4 | 5 | 4 | 4 | 4 | 4 | 4 | 4 | 4 | 4 | 4 | 3 | 5 | 25 | 64 |
| 120° | 25 | 6 | 5 | 6 | 6 | 5 | 4 | 3 | 3 | 3 | 3 | 3 | 3 | 3 | 3 | 5 | 25 | 64 |
|  | 29 | 9 | 11 | 12 | 9 | 6 | 3 | 3 | 3 | 3 | 3 | 3 | 3 | 3 | 2 | 4 | 24 | 64 |
|  | 32 | 21 | 25 | 21 | 11 | 5 | 3 | 2 | 2 | 2 | 2 | 2 | 2 | 2 | 2 | 4 | 24 | 66 |
|  | 52 | 49 | 43 | 25 | 10 | 3 | 1 | 1 | 1 | 1 | 2 | 2 | 2 | 1 | 1 | 4 | 27 | 75 |
|  | 94 | 79 | 46 | 18 | 6 | 2 | 1 | 1 | 1 | 1 | 1 | 1 | 1 | 1 | 1 | 7 | 37 | XX |
|  | XX | 73 | 29 | 9 | 2 | 1 | 0 | 0 | 0 | 0 | 0 | 0 | 0 | 1 | 4 | 17 | 65 | XX |
| 180° | XX | 41 | 13 | 3 | 1 | 0 | 0 | 0 | ● | 0 | 0 | 0 | 1 | 3 | 13 | 41 | XX | XX |

**Figure 5.** Relative conformation energies (in kcal/mol) for EEK with the constraints of $\theta_L = \theta_2 = \theta_R = \theta_{ee}$ and $\theta_1 = \theta_{ek}$. The filled circles (●) indicate absolute energy minima. The XX's indicate relative energies in excess of 100 kcal/mol. Values in the potential map have been rounded into integers.

similar to the case of DPE. Possible effects from electron delocalization are masked by the strong repulsion between the ortho hydrogen and the carbonyl oxygen and therefore not discernible. Only one type of large-amplitude ring motion, i.e., 180° flips, with a low barrier of ca. 2 kcal/mol may be identified. Again, this type of ring flip corresponds to minimized ring–ring repulsion.

**Equilibrium Positions of Phenylene Rings.** Given in Figure 5 is the potential map of EEK with the constraints of $\theta_1 = \theta_{ee}$ and $\theta_L = \theta_2 = \theta_R = \theta_{ek}$, where subscripts ee and ek denote ether–ether and ether–ketone rings, respectively.

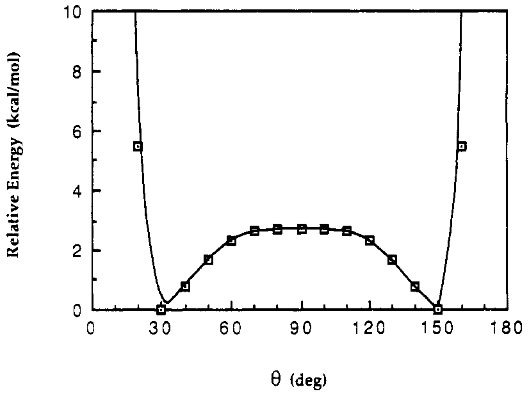

**Figure 6.** Relative conformation energy curve for EEK with the constraint of $\theta_L = \theta_1 = \theta_2 = \theta_R = \theta$.

The constraints are intended for the search of the conformation of lowest energy (i.e., the equilibrium angular positions of the aromatic rings) in PEEK with the consideration of structural identity of the phenylene rings. As may be observed in Figure 5, this equilibrium position lies at $(\theta_{ee},\theta_{ek}) = (0°,90°)$; i.e., the ether–ether rings prefer to lie on the molecular plane whereas the ether–ketone ring prefers to lie vertical to the plane of the backbone zigzag. This conformation is quite different from that (i.e., $\theta_{ee} = \theta_{ek} =$ ca. 40°) reported for PEEK chains in the crystalline state. The apparent discrepancy suggests the existence of strong *inter*molecular interactions in the crystalline PEEK which significantly exceed those which could be accounted for by the assumption of structural rigidity in our calculations.

The calculated energy minimum at $(\theta_{ee},\theta_{ek}) = (0°,90°)$ may probably be considered as representing the compar-

| $\theta_1$ \ $\theta_2$ | | | | | | | | | 90° | | | | | | | | | 180° | | | | | | | | | 270° | | | | | | | | | 360° |
|---|---|---|---|---|---|---|---|---|---|---|---|---|---|---|---|---|---|---|---|---|---|---|---|---|---|---|---|---|---|---|---|---|---|---|---|---|
| | 24 | 9 | 3 | 2 | 1 | 1 | 1 | 1 | 1 | 1 | 1 | 2 | 6 | 17 | 37 | 60 | 71 | 52 | 24 | 9 | 3 | 2 | 1 | 1 | 1 | 1 | 1 | 1 | 1 | 2 | 6 | 17 | 37 | 60 | 71 | 52 |
| | 9 | 2 | 0 | 0 | 0 | 0 | 0 | 0 | 0 | ● | 0 | 1 | 7 | 20 | 44 | 61 | 50 | 26 | 9 | 2 | 0 | 0 | 0 | 0 | 0 | 0 | 0 | ● | 0 | 1 | 7 | 20 | 44 | 61 | 50 | 26 |
| | 4 | 1 | 0 | 0 | 0 | 1 | 1 | 1 | 0 | 0 | 0 | 2 | 9 | 23 | 43 | 46 | 30 | 13 | 4 | 1 | 0 | 0 | 0 | 1 | 1 | 1 | 0 | 0 | 0 | 2 | 9 | 23 | 43 | 46 | 30 | 13 |
| | 3 | 1 | 1 | 1 | 1 | 2 | 1 | 1 | 1 | 1 | 1 | 3 | 10 | 22 | 34 | 33 | 20 | 8 | 3 | 1 | 1 | 1 | 1 | 2 | 1 | 1 | 1 | 1 | 1 | 3 | 10 | 22 | 34 | 33 | 20 | 8 |
| | 3 | 2 | 1 | 2 | 2 | 2 | 2 | 2 | 2 | 2 | 2 | 4 | 9 | 18 | 27 | 27 | 17 | 8 | 3 | 2 | 1 | 2 | 2 | 2 | 2 | 2 | 2 | 2 | 2 | 4 | 9 | 18 | 27 | 27 | 17 | 8 |
| | 4 | 2 | 2 | 2 | 2 | 2 | 2 | 2 | 2 | 2 | 3 | 4 | 8 | 15 | 24 | 25 | 17 | 8 | 4 | 2 | 2 | 2 | 2 | 2 | 2 | 2 | 2 | 2 | 3 | 4 | 8 | 15 | 24 | 25 | 17 | 8 |
| | 4 | 3 | 3 | 3 | 3 | 3 | 3 | 3 | 3 | 3 | 3 | 4 | 7 | 14 | 24 | 25 | 17 | 9 | 4 | 3 | 3 | 3 | 3 | 3 | 3 | 3 | 3 | 3 | 3 | 4 | 7 | 14 | 24 | 25 | 17 | 9 |
| | 4 | 3 | 3 | 3 | 3 | 3 | 3 | 3 | 3 | 3 | 3 | 4 | 7 | 14 | 24 | 26 | 17 | 9 | 4 | 3 | 3 | 3 | 3 | 3 | 3 | 3 | 3 | 3 | 3 | 4 | 7 | 14 | 24 | 26 | 17 | 9 |
| 90° | 5 | 3 | 3 | 3 | 3 | 3 | 3 | 3 | 3 | 3 | 3 | 4 | 7 | 14 | 24 | 26 | 17 | 9 | 5 | 3 | 3 | 3 | 3 | 3 | 3 | 3 | 3 | 3 | 3 | 4 | 7 | 14 | 24 | 26 | 17 | 9 |
| | 4 | 3 | 3 | 3 | 3 | 3 | 3 | 3 | 3 | 3 | 3 | 4 | 7 | 14 | 24 | 26 | 17 | 9 | 4 | 3 | 3 | 3 | 3 | 3 | 3 | 3 | 3 | 3 | 3 | 4 | 7 | 14 | 24 | 26 | 17 | 9 |
| | 4 | 3 | 3 | 3 | 3 | 3 | 3 | 3 | 3 | 3 | 3 | 4 | 7 | 14 | 24 | 27 | 17 | 9 | 4 | 3 | 3 | 3 | 3 | 3 | 3 | 3 | 3 | 3 | 3 | 4 | 7 | 14 | 24 | 27 | 17 | 9 |
| | 5 | 4 | 4 | 5 | 5 | 4 | 4 | 3 | 3 | 3 | 3 | 4 | 7 | 15 | 24 | 26 | 18 | 9 | 5 | 4 | 4 | 5 | 5 | 4 | 4 | 3 | 3 | 3 | 3 | 4 | 7 | 15 | 24 | 26 | 18 | 9 |
| | 8 | 8 | 10 | 11 | 9 | 8 | 7 | 6 | 6 | 6 | 6 | 7 | 10 | 17 | 27 | 29 | 20 | 12 | 8 | 8 | 10 | 11 | 9 | 8 | 7 | 6 | 6 | 6 | 6 | 7 | 10 | 17 | 27 | 29 | 20 | 12 |
| | 12 | 22 | 24 | 22 | 17 | 14 | 13 | 13 | 13 | 13 | 13 | 13 | 17 | 24 | 34 | 35 | 27 | 20 | 12 | 22 | 24 | 22 | 17 | 14 | 13 | 13 | 13 | 13 | 13 | 13 | 17 | 24 | 34 | 35 | 27 | 20 |
| | 38 | 44 | 42 | 33 | 26 | 23 | 22 | 22 | 21 | 21 | 22 | 23 | 26 | 33 | 43 | 45 | 38 | 34 | 38 | 44 | 42 | 33 | 26 | 23 | 22 | 22 | 21 | 21 | 22 | 23 | 26 | 33 | 43 | 45 | 38 | 34 |
| | 60 | 61 | 45 | 31 | 25 | 23 | 23 | 23 | 23 | 22 | 23 | 23 | 27 | 34 | 44 | 48 | 45 | 48 | 60 | 61 | 45 | 31 | 25 | 23 | 23 | 23 | 23 | 22 | 23 | 23 | 27 | 34 | 44 | 48 | 45 | 48 |
| | 71 | 50 | 29 | 18 | 15 | 14 | 14 | 14 | 14 | 14 | 14 | 15 | 18 | 26 | 37 | 44 | 50 | 65 | 71 | 50 | 29 | 18 | 15 | 14 | 14 | 14 | 14 | 14 | 14 | 15 | 18 | 26 | 37 | 44 | 50 | 65 |
| 180° | 52 | 25 | 12 | 7 | 6 | 6 | 6 | 6 | 6 | 5 | 5 | 6 | 10 | 18 | 33 | 48 | 65 | 74 | 52 | 25 | 12 | 7 | 6 | 6 | 6 | 6 | 6 | 5 | 5 | 6 | 10 | 18 | 33 | 48 | 65 | 74 |
| | 24 | 9 | 3 | 2 | 1 | 1 | 1 | 1 | 1 | 1 | 1 | 2 | 6 | 17 | 37 | 60 | 71 | 52 | 24 | 9 | 3 | 2 | 1 | 1 | 1 | 1 | 1 | 1 | 1 | 2 | 6 | 17 | 37 | 60 | 71 | 52 |
| | 9 | 2 | 0 | 0 | 0 | 0 | 0 | 0 | 0 | ● | 0 | 1 | 7 | 20 | 44 | 61 | 50 | 26 | 9 | 2 | 0 | 0 | 0 | 0 | 0 | 0 | 0 | ● | 0 | 1 | 7 | 20 | 44 | 61 | 50 | 26 |
| | 4 | 1 | 0 | 0 | 0 | 1 | 1 | 1 | 0 | 0 | 0 | 2 | 9 | 23 | 43 | 46 | 30 | 13 | 4 | 1 | 0 | 0 | 0 | 1 | 1 | 1 | 0 | 0 | 0 | 2 | 9 | 23 | 43 | 46 | 30 | 13 |
| | 3 | 1 | 1 | 1 | 1 | 2 | 1 | 1 | 1 | 1 | 1 | 3 | 10 | 22 | 34 | 33 | 20 | 8 | 3 | 1 | 1 | 1 | 1 | 2 | 1 | 1 | 1 | 1 | 1 | 3 | 10 | 22 | 34 | 33 | 20 | 8 |
| | 3 | 2 | 1 | 2 | 2 | 2 | 2 | 2 | 2 | 2 | 2 | 4 | 9 | 18 | 27 | 27 | 17 | 8 | 3 | 2 | 1 | 2 | 2 | 2 | 2 | 2 | 2 | 2 | 2 | 4 | 9 | 18 | 27 | 27 | 17 | 8 |
| | 4 | 2 | 2 | 2 | 2 | 2 | 2 | 2 | 2 | 2 | 3 | 4 | 8 | 15 | 24 | 25 | 17 | 8 | 4 | 2 | 2 | 2 | 2 | 2 | 2 | 2 | 2 | 2 | 3 | 4 | 8 | 15 | 24 | 25 | 17 | 8 |
| | 4 | 3 | 3 | 3 | 3 | 3 | 3 | 3 | 3 | 3 | 3 | 4 | 7 | 14 | 24 | 25 | 17 | 9 | 4 | 3 | 3 | 3 | 3 | 3 | 3 | 3 | 3 | 3 | 3 | 4 | 7 | 14 | 24 | 25 | 17 | 9 |
| | 4 | 3 | 3 | 3 | 3 | 3 | 3 | 3 | 3 | 3 | 3 | 4 | 7 | 14 | 24 | 26 | 17 | 9 | 4 | 3 | 3 | 3 | 3 | 3 | 3 | 3 | 3 | 3 | 3 | 4 | 7 | 14 | 24 | 26 | 17 | 9 |
| 270° | 5 | 3 | 3 | 3 | 3 | 3 | 3 | 3 | 3 | 3 | 3 | 4 | 7 | 14 | 24 | 26 | 17 | 9 | 5 | 3 | 3 | 3 | 3 | 3 | 3 | 3 | 3 | 3 | 3 | 4 | 7 | 14 | 24 | 26 | 17 | 9 |
| | 4 | 3 | 3 | 3 | 3 | 3 | 3 | 3 | 3 | 3 | 3 | 4 | 7 | 14 | 24 | 26 | 17 | 9 | 4 | 3 | 3 | 3 | 3 | 3 | 3 | 3 | 3 | 3 | 3 | 4 | 7 | 14 | 24 | 26 | 17 | 9 |
| | 4 | 3 | 3 | 3 | 3 | 3 | 3 | 3 | 3 | 3 | 3 | 4 | 7 | 14 | 24 | 27 | 17 | 9 | 4 | 3 | 3 | 3 | 3 | 3 | 3 | 3 | 3 | 3 | 3 | 4 | 7 | 14 | 24 | 27 | 17 | 9 |
| | 5 | 4 | 4 | 5 | 5 | 4 | 4 | 3 | 3 | 3 | 3 | 4 | 7 | 15 | 24 | 26 | 18 | 9 | 5 | 4 | 4 | 5 | 5 | 4 | 4 | 3 | 3 | 3 | 3 | 4 | 7 | 15 | 24 | 26 | 18 | 9 |
| | 8 | 8 | 10 | 11 | 9 | 8 | 7 | 6 | 6 | 6 | 6 | 7 | 10 | 17 | 27 | 29 | 20 | 12 | 8 | 8 | 10 | 11 | 9 | 8 | 7 | 6 | 6 | 6 | 6 | 7 | 10 | 17 | 27 | 29 | 20 | 12 |
| | 12 | 22 | 24 | 22 | 17 | 14 | 13 | 13 | 13 | 13 | 13 | 13 | 17 | 24 | 34 | 35 | 27 | 20 | 12 | 22 | 24 | 22 | 17 | 14 | 13 | 13 | 13 | 13 | 13 | 13 | 17 | 24 | 34 | 35 | 27 | 20 |
| | 38 | 44 | 42 | 33 | 26 | 23 | 22 | 22 | 21 | 21 | 22 | 23 | 26 | 33 | 43 | 45 | 38 | 34 | 38 | 44 | 42 | 33 | 26 | 23 | 22 | 22 | 21 | 21 | 22 | 23 | 26 | 33 | 43 | 45 | 38 | 34 |
| | 60 | 61 | 45 | 31 | 25 | 23 | 23 | 23 | 23 | 22 | 23 | 23 | 27 | 34 | 44 | 48 | 45 | 48 | 60 | 61 | 45 | 31 | 25 | 23 | 23 | 23 | 23 | 22 | 23 | 23 | 27 | 34 | 44 | 48 | 45 | 48 |
| | 71 | 50 | 29 | 18 | 15 | 14 | 14 | 14 | 14 | 14 | 14 | 15 | 18 | 26 | 37 | 44 | 50 | 65 | 71 | 50 | 29 | 18 | 15 | 14 | 14 | 14 | 14 | 14 | 14 | 15 | 18 | 26 | 37 | 44 | 50 | 65 |
| 360° | 52 | 25 | 12 | 7 | 6 | 6 | 6 | 6 | 6 | 5 | 5 | 6 | 10 | 18 | 33 | 48 | 65 | 74 | 52 | 25 | 12 | 7 | 6 | 6 | 6 | 6 | 6 | 5 | 5 | 6 | 10 | 18 | 33 | 48 | 65 | 74 |

**Figure 7.** Relative conformation energies (in kcal/mol) for EEK with the constraint of $\theta_L = \theta_R = 30°$. The filled circles (●) indicate absolute energy minima. Values in the potential map have been rounded into integers.

atively more populated conformation in the amorphous PEEK. Interestingly, $\theta_{ek}$ may be moderately altered (say, in the range of 90 ± 35°) without significant increase in potential energy; i.e., the ether–ketone rings in the amorphous phase may possess a relatively wide range of angular positions. In comparison, $\theta_{ee}$ is restricted (say, in the range of 0 ± 15°), suggesting the limited distribution of angular positions for ether–ether rings in the amorphous state. The ether–ether ring appears capable of a 180° flip (with a barrier of ca. 4 kcal/mol), which is equivalent to two of the 180° flips in DPE or DPK.

To facilitate further comparison, a more stringent constraint based on the experimental observation of $\theta_L = \theta_1 = \theta_2 = \theta_R = \theta$ (i.e., $\theta_{ee} = \theta_{ek} = \theta$) may be imposed. The corresponding potential curve is given in Figure 6, which actually corresponds to the diagonal cross-section of Figure 5. The equilibrium position is now at $\theta = 30°$, in reasonable agreement with the experimental value of ca. 40°. This indicates that efficient packing of rings (facilitated understandably by the fixed tilt angle of the phenylene rings) in the crystalline state is indeed the source of the strong intermolecular interactions.

In an earlier Fourier-transform infrared spectroscopic (FTIR) study of PEEK, Nguyen and Ishida[33] observed that the carbonyl stretching frequency shifts from 1655 to 1648 $\text{cm}^{-1}$ upon crystallization. They attributed this red shift to the movement of ether–ketone rings to approach coplanarity upon crystallization. This is consistent with the present results for the change of preferred tilt angle of the ether–ketone ring from ca. 90 ± 35° to ca. 30°. The FTIR observations of Nguyen and Ishida[33] also indicated the presence of local order around ether–ether rings in the melt state at 380 °C (some 40 °C above the observed melting point but below the reported equilibrium melting temperature of 395 °C). The dissipation of this local order required heat treatment at 400 °C. Partial alignment of molecular chains in amorphous PEEK prepared by rapid quenching has also been proposed by Sasuga and Hagiwara.[16] For high polymers, it is well-known that local order inherited from the crystalline state may be retained after melting of the crystal.[34] Depending on the melt temperature, this local order may persist for a considerable period of time. (In the FTIR study of Nguyen and Ishida, the annealing time at 380 °C was 10 min.) Consistent with their observation, our results indicate a more limited range of preferred angular positions (i.e., 0 ± 15°) for ether–ether rings, which are therefore likely to possess or retain local order in the amorphous state.

**Rotation of Phenylene Rings in the Crystalline State.** Given in Figure 7 is the potential map of EEK with the constraint of $\theta_L = \theta_R = 30°$. This is intended to simulate the crystalline phase in PEEK. The selection of a tilt angle of 30° (instead of the slightly different value of 40° observed from X-ray diffraction analysis) is for the sake of consistency in our calculations. General features of the potential map are not altered by this slight change in the inclination angle. As may be observed, the absolute energy mimina correspond to $(\theta_1,\theta_2) = (20°,100°)$ or the equivalent, quite apart from the experimentally determined inclination angle of ca. 40° or the calculated inclination angle of 30° for crystalline PEEK. However, the relative energy at $(\theta_1,\theta_2) = (30°,30°)$ is fairly small (only ca. 0.2 kcal/mol) and well within the level of thermal energy (i.e., 0.6 kcal/mol) at room temperature. The ether–ketone ring appears moderately mobile, capable of moving freely in the angular range of $\theta_2 = 70 \pm 45°$ at room tem-

| $\theta_2$ $\theta_1$ | | | | | | | | | 90° | | | | | | | | | 180° | | | | | | | | | 270° | | | | | | | | | 360° |
|---|---|---|---|---|---|---|---|---|---|---|---|---|---|---|---|---|---|---|---|---|---|---|---|---|---|---|---|---|---|---|---|---|---|---|---|---|
| | 22 | 8 | 2 | 1 | 0 | 0 | 0 | 0 | 0 | 0 | 0 | 0 | 1 | 5 | 15 | 36 | 55 | 45 | 22 | 8 | 2 | 1 | 0 | 0 | 0 | 0 | 0 | 0 | 0 | 0 | 1 | 5 | 15 | 36 | 55 | 45 |
| | 8 | 3 | 1 | 1 | 1 | 1 | 1 | 1 | 1 | 1 | 1 | 1 | 3 | 9 | 24 | 39 | 37 | 21 | 8 | 3 | 1 | 1 | 1 | 1 | 1 | 1 | 1 | 1 | 1 | 1 | 3 | 9 | 24 | 39 | 37 | 21 |
| | 3 | 2 | 1 | 1 | 1 | 1 | 1 | 1 | 1 | 1 | 1 | 2 | 5 | 13 | 22 | 24 | 16 | 8 | 3 | 2 | 1 | 1 | 1 | 1 | 1 | 1 | 1 | 1 | 1 | 2 | 5 | 13 | 22 | 24 | 16 | 8 |
| | 3 | 2 | 2 | 2 | 2 | 2 | 2 | 2 | 2 | 2 | 2 | 3 | 7 | 11 | 14 | 11 | 7 | 4 | 3 | 2 | 2 | 2 | 2 | 2 | 2 | 2 | 2 | 2 | 2 | 3 | 7 | 11 | 14 | 11 | 7 | 4 |
| | 3 | 3 | 3 | 3 | 3 | 3 | 3 | 3 | 3 | 3 | 3 | 4 | 6 | 7 | 7 | 5 | 4 | 3 | 3 | 3 | 3 | 3 | 3 | 3 | 3 | 3 | 3 | 3 | 3 | 4 | 6 | 7 | 7 | 5 | 4 | 3 |
| | 3 | 3 | 3 | 3 | 3 | 3 | 3 | 3 | 3 | 3 | 3 | 4 | 5 | 5 | 4 | 4 | 3 | 3 | 3 | 3 | 3 | 3 | 3 | 3 | 3 | 3 | 3 | 3 | 3 | 4 | 5 | 5 | 4 | 4 | 3 | 3 |
| | 4 | 4 | 4 | 4 | 4 | 4 | 4 | 4 | 4 | 4 | 4 | 4 | 4 | 4 | 4 | 4 | 4 | 4 | 4 | 4 | 4 | 4 | 4 | 4 | 4 | 4 | 4 | 4 | 4 | 4 | 4 | 4 | 4 | 4 | 4 | 4 |
| | 4 | 4 | 4 | 4 | 4 | 4 | 4 | 4 | 4 | 4 | 4 | 4 | 4 | 4 | 4 | 4 | 4 | 4 | 4 | 4 | 4 | 4 | 4 | 4 | 4 | 4 | 4 | 4 | 4 | 4 | 4 | 4 | 4 | 4 | 4 | 4 |
| 90° | 4 | 4 | 4 | 4 | 4 | 4 | 4 | 4 | 4 | 4 | 4 | 4 | 4 | 4 | 4 | 4 | 4 | 4 | 4 | 4 | 4 | 4 | 4 | 4 | 4 | 4 | 4 | 4 | 4 | 4 | 4 | 4 | 4 | 4 | 4 | 4 |
| | 4 | 4 | 4 | 4 | 4 | 4 | 4 | 4 | 4 | 4 | 4 | 4 | 4 | 4 | 4 | 4 | 4 | 4 | 4 | 4 | 4 | 4 | 4 | 4 | 4 | 4 | 4 | 4 | 4 | 4 | 4 | 4 | 4 | 4 | 4 | 4 |
| | 4 | 4 | 4 | 4 | 4 | 4 | 4 | 4 | 4 | 4 | 4 | 4 | 4 | 4 | 4 | 4 | 4 | 4 | 4 | 4 | 4 | 4 | 4 | 4 | 4 | 4 | 4 | 4 | 4 | 4 | 4 | 4 | 4 | 4 | 4 | 4 |
| | 3 | 4 | 4 | 5 | 5 | 4 | 3 | 3 | 3 | 3 | 3 | 3 | 3 | 3 | 3 | 3 | 3 | 3 | 3 | 4 | 4 | 5 | 5 | 4 | 3 | 3 | 3 | 3 | 3 | 3 | 3 | 3 | 3 | 3 | 3 | 3 |
| | 4 | 5 | 7 | 7 | 6 | 4 | 3 | 3 | 3 | 3 | 3 | 3 | 3 | 3 | 3 | 3 | 3 | 3 | 4 | 5 | 7 | 7 | 6 | 4 | 3 | 3 | 3 | 3 | 3 | 3 | 3 | 3 | 3 | 3 | 3 | 3 |
| | 7 | 11 | 14 | 11 | 7 | 3 | 2 | 2 | 2 | 2 | 2 | 2 | 2 | 2 | 2 | 2 | 3 | 4 | 7 | 11 | 14 | 11 | 7 | 3 | 2 | 2 | 2 | 2 | 2 | 2 | 2 | 2 | 2 | 2 | 3 | 4 |
| | 16 | 24 | 22 | 13 | 5 | 2 | 1 | 1 | 1 | 1 | 1 | 1 | 1 | 1 | 1 | 2 | 3 | 8 | 16 | 24 | 22 | 13 | 5 | 2 | 1 | 1 | 1 | 1 | 1 | 1 | 1 | 1 | 1 | 2 | 3 | 8 |
| | 37 | 39 | 24 | 9 | 3 | 1 | 1 | 1 | 1 | 1 | 1 | 1 | 1 | 1 | 1 | 3 | 8 | 21 | 37 | 39 | 24 | 9 | 3 | 1 | 1 | 1 | 1 | 1 | 1 | 1 | 1 | 1 | 1 | 3 | 8 | 21 |
| | 55 | 36 | 15 | 5 | 1 | 0 | 0 | 0 | 0 | 0 | 0 | 0 | 0 | 1 | 2 | 8 | 22 | 45 | 55 | 36 | 15 | 5 | 1 | 0 | 0 | 0 | 0 | 0 | 0 | 0 | 0 | 1 | 2 | 8 | 22 | 45 |
| 180° | 45 | 20 | 6 | 2 | 0 | 0 | 0 | 0 | ● | 0 | 0 | 0 | 0 | 2 | 6 | 20 | 45 | 62 | 45 | 20 | 6 | 2 | 0 | 0 | 0 | 0 | ● | 0 | 0 | 0 | 0 | 2 | 6 | 20 | 45 | 62 |
| | 22 | 8 | 2 | 1 | 0 | 0 | 0 | 0 | 0 | 0 | 0 | 0 | 1 | 5 | 15 | 36 | 55 | 45 | 22 | 8 | 2 | 1 | 0 | 0 | 0 | 0 | 0 | 0 | 0 | 0 | 1 | 5 | 15 | 36 | 55 | 45 |
| | 8 | 3 | 1 | 1 | 1 | 1 | 1 | 1 | 1 | 1 | 1 | 1 | 3 | 9 | 24 | 39 | 37 | 21 | 8 | 3 | 1 | 1 | 1 | 1 | 1 | 1 | 1 | 1 | 1 | 1 | 3 | 9 | 24 | 39 | 37 | 21 |
| | 3 | 2 | 1 | 1 | 1 | 1 | 1 | 1 | 1 | 1 | 1 | 2 | 5 | 13 | 22 | 24 | 16 | 8 | 3 | 2 | 1 | 1 | 1 | 1 | 1 | 1 | 1 | 1 | 1 | 2 | 5 | 13 | 22 | 24 | 16 | 8 |
| | 3 | 2 | 2 | 2 | 2 | 2 | 2 | 2 | 2 | 2 | 2 | 3 | 7 | 11 | 14 | 11 | 7 | 4 | 3 | 2 | 2 | 2 | 2 | 2 | 2 | 2 | 2 | 2 | 2 | 3 | 7 | 11 | 14 | 11 | 7 | 4 |
| | 3 | 3 | 3 | 3 | 3 | 3 | 3 | 3 | 3 | 3 | 3 | 4 | 6 | 7 | 7 | 5 | 4 | 3 | 3 | 3 | 3 | 3 | 3 | 3 | 3 | 3 | 3 | 3 | 3 | 4 | 6 | 7 | 7 | 5 | 4 | 3 |
| | 3 | 3 | 3 | 3 | 3 | 3 | 3 | 3 | 3 | 3 | 3 | 4 | 5 | 5 | 4 | 4 | 3 | 3 | 3 | 3 | 3 | 3 | 3 | 3 | 3 | 3 | 3 | 3 | 3 | 4 | 5 | 5 | 4 | 4 | 3 | 3 |
| | 4 | 4 | 4 | 4 | 4 | 4 | 4 | 4 | 4 | 4 | 4 | 4 | 4 | 4 | 4 | 4 | 4 | 4 | 4 | 4 | 4 | 4 | 4 | 4 | 4 | 4 | 4 | 4 | 4 | 4 | 4 | 4 | 4 | 4 | 4 | 4 |
| | 4 | 4 | 4 | 4 | 4 | 4 | 4 | 4 | 4 | 4 | 4 | 4 | 4 | 4 | 4 | 4 | 4 | 4 | 4 | 4 | 4 | 4 | 4 | 4 | 4 | 4 | 4 | 4 | 4 | 4 | 4 | 4 | 4 | 4 | 4 | 4 |
| 270° | 4 | 4 | 4 | 4 | 4 | 4 | 4 | 4 | 4 | 4 | 4 | 4 | 4 | 4 | 4 | 4 | 4 | 4 | 4 | 4 | 4 | 4 | 4 | 4 | 4 | 4 | 4 | 4 | 4 | 4 | 4 | 4 | 4 | 4 | 4 | 4 |
| | 4 | 4 | 4 | 4 | 4 | 4 | 4 | 4 | 4 | 4 | 4 | 4 | 4 | 4 | 4 | 4 | 4 | 4 | 4 | 4 | 4 | 4 | 4 | 4 | 4 | 4 | 4 | 4 | 4 | 4 | 4 | 4 | 4 | 4 | 4 | 4 |
| | 4 | 4 | 4 | 4 | 4 | 4 | 4 | 4 | 4 | 4 | 4 | 4 | 4 | 4 | 4 | 4 | 4 | 4 | 4 | 4 | 4 | 4 | 4 | 4 | 4 | 4 | 4 | 4 | 4 | 4 | 4 | 4 | 4 | 4 | 4 | 4 |
| | 3 | 4 | 4 | 5 | 5 | 4 | 3 | 3 | 3 | 3 | 3 | 3 | 3 | 3 | 3 | 3 | 3 | 3 | 3 | 4 | 4 | 5 | 5 | 4 | 3 | 3 | 3 | 3 | 3 | 3 | 3 | 3 | 3 | 3 | 3 | 3 |
| | 4 | 5 | 7 | 7 | 6 | 4 | 3 | 3 | 3 | 3 | 3 | 3 | 3 | 3 | 3 | 3 | 3 | 3 | 4 | 5 | 7 | 7 | 6 | 4 | 3 | 3 | 3 | 3 | 3 | 3 | 3 | 3 | 3 | 3 | 3 | 3 |
| | 7 | 11 | 14 | 11 | 7 | 3 | 2 | 2 | 2 | 2 | 2 | 2 | 2 | 2 | 2 | 2 | 3 | 4 | 7 | 11 | 14 | 11 | 7 | 3 | 2 | 2 | 2 | 2 | 2 | 2 | 2 | 2 | 2 | 2 | 3 | 4 |
| | 16 | 24 | 22 | 13 | 5 | 2 | 1 | 1 | 1 | 1 | 1 | 1 | 1 | 1 | 1 | 2 | 3 | 8 | 16 | 24 | 22 | 13 | 5 | 2 | 1 | 1 | 1 | 1 | 1 | 1 | 1 | 1 | 1 | 2 | 3 | 8 |
| | 37 | 39 | 24 | 9 | 3 | 1 | 1 | 1 | 1 | 1 | 1 | 1 | 1 | 1 | 1 | 3 | 8 | 21 | 37 | 39 | 24 | 9 | 3 | 1 | 1 | 1 | 1 | 1 | 1 | 1 | 1 | 1 | 1 | 3 | 8 | 21 |
| | 55 | 36 | 15 | 5 | 1 | 0 | 0 | 0 | 0 | 0 | 0 | 0 | 0 | 1 | 2 | 8 | 22 | 45 | 55 | 36 | 15 | 5 | 1 | 0 | 0 | 0 | 0 | 0 | 0 | 0 | 0 | 1 | 2 | 8 | 22 | 45 |
| 360° | 45 | 20 | 6 | 2 | 0 | 0 | 0 | 0 | ● | 0 | 0 | 0 | 0 | 2 | 6 | 20 | 45 | 62 | 45 | 20 | 6 | 2 | 0 | 0 | 0 | 0 | ● | 0 | 0 | 0 | 0 | 2 | 6 | 20 | 45 | 62 |

**Figure 8.** Relative conformation energies (in kcal/mol) for EEK with the constraint of $\theta_L = 0°$ and $\theta_R = 90°$. The filled circles (●) indicate absolute energy minima. Values in the potential map have been rounded into integers.

perature; in comparison, the ether–ether ring is more restricted at room temperature, limited to $\theta_1 = 25 \pm 10°$. In addition, a 180° flip of the ether–ether ring (but not the ether–ketone ring) appears possible. The barrier, however, is quite high (in the vicinity of 22 kcal/mol) but probably not high enough to be prohibitive. Some of the observations above are contradictory to previous solid-state NMR results.[20,21] To reconcile the discrepancies, the following arguments are proposed.

Due to geometric reasons, a phenylene ring may be subjected to stronger *inter*molecular repulsion when it is vertical to the plane of the main-chain zigzag. We suggest that, due to the additional intermolecular interactions involved, the actual relative energy in the vicinity of this conformation should be somewhat higher than that calculated. If angular positions within the range of, say, $(\theta_1,\theta_2) = (90\pm40°,90\pm40°)$ are assumed to be significantly affected by the *inter*molecular interactions, there should then be additional contributions to the relative energies than those indicated in Figure 7 in this angular range. This modification would therefore drastically limit the amplitude of the ether–ketone ring motion and bring the equilibrium position to the vicinity of $(\theta_1,\theta_2) = (30°,30°)$. Flipping of the ether–ether ring would also become prohibited. The immobility of the phenylene rings may therefore be interpreted as a result of both *intra*molecular interactions resisting the coplanar conformation and *inter*molecular interactions most operative when the ring is vertical to the plane to the zigzagging virtual bonds.

**Rotation of Phenylene Rings in the Amorphous State.** Given in Figure 8 is the potential map of EEK with the constraint that $\theta_L = 0°$ and $\theta_R = 90°$, which should correspond approximately to the case of amorphous PEEK. The mobility of the phenylene rings in this case is clearly better than that in Figure 7. Apparent possibilities of ring movement include limited oscillation of the ether–ether phenylene in the range of $\theta_1 = 0 \pm 15°$, moderate oscillation of the ether–ketone phenylene in the range of $\theta_2 = 90 \pm 45°$, 180° flip of the ether–ether ring, and synchronous rotation of both rings. In each of the latter two cases, the corresponding activation energy is ca. 4 kcal/mol, equivalent to two of the ring flips in DPE or DPK. These features are in general agreement with the previous solid-state NMR results.[20,21] Specifically, the calculated barrier for the 180° flip of the ether–ether ring is 3.8 kcal/mol, in reasonable agreement the value of 3.2 kcal/mol estimated from the temperature dependence of the spin-lattice relaxation time in the wide-line $^1$H NMR study by Clark et al.[20] However, there exists one major disagreement: the ether–ketone ring in Figure 8 is not capable of the 180° flip (although reportedly limited to only 25% of the population) suggested by Poliks and Schaefer[21] in their CP/MAS $^{13}$C NMR study. We are not able to provide explanations for this discrepancy at the present time.

**Molecular Mechanism of γ-Relaxation.** Before extending our discussion to segmental motion in PEEK, it is necessary to recognize that, although the calculations here are for the rotation of phenylene rings with the virtual bonds (i.e., the $C_2$ axes of the phenylenes) fixed, the potential maps of DPE and DPK are equivalent to torsional motion of the virtual bonds with the phenylene rings fixed (i.e., "glued") to the virtual bonds.

Given in Figures 9 and 10 are two possible modes of backbone motion in PEEK; both are of the crankshaft type. To avoid excessive hindrance from surrounding rings in the glassy matrix, phenylene rings in the rotating virtual

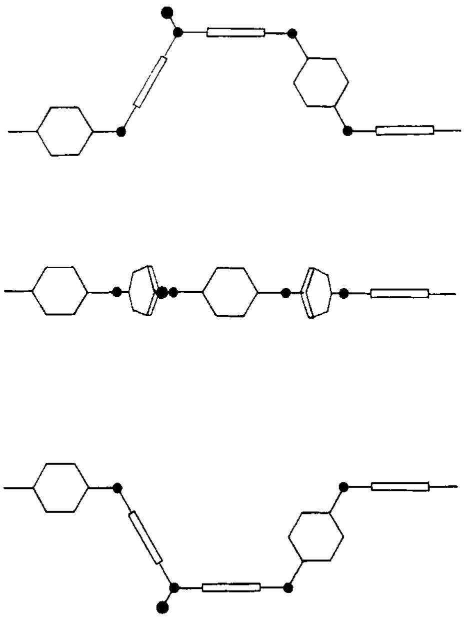

**Figure 9.** The first mode of crankshaft motion proposed for the $\gamma$-relaxation in PEEK. The pivoting points correspond to an ether linkage and a ketone linkage.

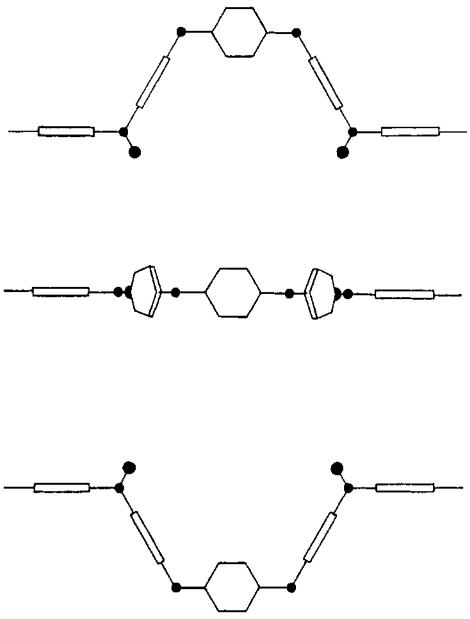

**Figure 10.** The second mode of crankshaft motion proposed for the $\gamma$-relaxation in PEEK. The pivoting points correspond to two ketone linkages.

bonds are assumed capable of adjusting themselves to stay perpendicular to the plane of rotating virtual bonds (i.e., the "crank") so that the cross-sectional area of the moving crank is kept small and therefore *inter*molecular interactions are minimized. The first mode of crankshaft motion is equivalent to four of the (0°,90°) to (180°,90°) flip in DPE discussed earlier. Each of these flips corresponds to a (sub)barrier of ca. 2 kcal/mol according to Figure 3. Under the assumption that these four subbarriers are simultaneous surmounted, the total barrier to this process is ca. 8 kcal/mol. The second mode of motion is equivalent to two of the (0°,90°) to (180°,90°) flip in DPE and two of the (90°,90°) to (270°,90°) flip in DPK. Since the barrier to the ring flip in DPK is also ca. 2 kcal/mol, the resulting total barrier is again ca. 8 kcal/mol.

The estimated barrier of ca. 8 kcal/mol for both modes is much smaller than the reported activation energy of ca. 21 kcal/mol determined from dynamic mechanical measurements[18] but in better agreement with the value of ca. 10 kcal/mol measured via dielectric means[18] for the $\gamma$-relaxation of PEEK. Since the mechanisms proposed above minimize intermolecular interactions, they are considered within the meaning of noncooperativity in the analysis of Starkweather and Avakian.[18]

## Conclusions

It is demonstrated via CNDO calculations for model compounds that ether–ether phenylene rings prefer to lie coplanar with, whereas ether–ketone rings prefer to lie vertical to, the PEEK backbone. This preferred arrangement of rings results in low intramolecular hindrance for medium- to large-amplitude rotational motion of phenylene rings or torsional motion of virtual bonds in the amorphous phase. In the crystalline state, phenylene rings give away their preferred angular positions and incline at a low angle from the backbone zigzag in an alternating manner to achieve efficient packing. The tight packing in the crystalline state results in strong intermolecular interactions which, in combination with the increased intramolecular hindrance (due to stronger repulsion between neighboring rings at the low tilt angle), prohibit movement of phenylene rings. These observations are in general agreement with results from earlier solid-state NMR studies.[20,21]

Local motions (presumably in the amorphous phase) of the crankshaft type were found to have potential barriers in the vicinity of 8 kcal/mol, in fair agreement with the activation energy of ca. 10 kcal/mol determined by dielectric means[18] but much lower than that of ca. 21 kcal/mol estimated from dynamic mechanical measurements[18] for the $\gamma$-relaxation of PEEK.

**Acknowledgment.** Thanks are due to the Computer Center of NSYSU for the help received during this work. This study is financially supported by the National Science Council, R.O.C., under Contract No. NSC80-0208-M110-11.

## References and Notes

(1) Cattanach, J. B.; Cogswell, F. N. In *Developments in Reinforced Plastics—5*; Pritchard, G., Ed.; Applied Science (Elsevier): New York, 1986; Chapter 1.
(2) Rigby, R. B. *Polym. News* **1984**, *9*, 325.
(3) Blundell, D. J.; Osborn, B. N. *SAMPE Q.* **1986**, *17*, 1.
(4) Cebe, P.; Hong, S. D. *Polymer* **1986**, *27*, 1183.
(5) Veslisaris, C. N.; Seferis, J. C. *Polym. Eng. Sci.* **1986**, *22*, 1574.
(6) Downs, R. J.; Berglund, L. A. *J. Reinf. Plast. Compos.* **1987**, *6*, 89.
(7) Chang, S.-S. *Polym. Commun.* **1988**, *29*, 138.
(8) Hsiung, C.-M.; Cakmak, M.; White, J. L. *Polym. Eng. Sci.* **1990**, *30*, 967.
(9) Spahr, D. E.; Schultz, J. M. *Polym. Compos.* **1990**, *11*, 201.
(10) Dawson, P. C.; Blundell, D. J. *Polymer* **1980**, *21*, 577.
(11) Rueda, D. R.; Ania, F.; Richardson, A.; Ward, I. M.; Calleja, F. J. B. *Polym. Commun.* **1983**, *24*, 258.
(12) Hay, J. N.; Kemmish, D. J.; Langford, J. I.; Rae, A. I. M. *Polym. Commun.* **1984**, *25*, 175.
(13) Attwood, T. E.; Dawson, P. C.; Freeman, J. L.; Hay, L. R. J.; Rose, L. B.; Staniland, P. A. *Polymer* **1981**, *22*, 1096.
(14) Karger-Kocsis, J.; Friedrich, K. *Polymer* **1986**, *27*, 1753.
(15) Chu, J.-N.; Schultz, J. M. *J. Mater. Sci.* **1990**, *25*, 3746.
(16) Sasuga, T.; Hagiwara, M. *Polymer* **1985**, *26*, 501.
(17) Sasuga, T.; Hagiwara, M. *Polymer* **1986**, *27*, 821.
(18) Starkweather, H. W., Jr.; Avakian, P. *Macromolecules* **1989**, *22*, 4060.
(19) Goodwin, A. A.; Hay, J. N. *Polym. Commun.* **1989**, *30*, 288.
(20) Clark, J. N.; Jagannathan, N. R.; Herring, F. G. *Polymer* **1988**, *29*, 341.
(21) Poliks, M. D.; Schaefer, J. *Macromolecules* **1990**, *23*, 3426.
(22) Sung, Y. J.; Chen, C. L.; Su, A. C. *Macromolecules* **1990**, *23*, 1941.

(23) Sung, Y. J.; Chen, C. L.; Su, A. C. *Macromolecules* **1991**, *24*, 6123.

(24) Hay, J. N.; Kemmish, D. J. *Polym. Commun.* **1989**, *30*, 77.

(25) Hay, J. N.; Langford, J. I.; Lloyd, J. R. *Polymer* **1989**, *30*, 489.

(26) Pople, J. A.; Beveridge, D. L. *Approximate Molecular Orbital Theory*; McGraw-Hill: New York, 1970.

(27) Sung, Y. J.; Chen, C. L.; Su, A. C. *Comput. Polym. Sci.*, submitted.

(28) Cowie, J. M. G.; Ferguson, R. *Polymer* **1987**, *28*, 503.

(29) Heijboer, J.; Baas, J. M. A.; van de Graaf, B.; Hoefnagel, M. A. *Polymer* **1987**, *28*, 509.

(30) Yannas, I. V.; Luise, R. R. *J. Macromol. Sci., Phys.* **1982**, *B21*, 443.

(31) Roy, A. K.; JOnes, A. A.; Inglefield, P. T. *Macromolecules* **1986**, *19*, 1356.

(32) Walton, J. H.; Lizak, M. J.; Conradi, M. S.; Gullion, T.; Schaefer, J. *Macromolecules* **1990**, *23*, 416.

(33) Nguyen, H. X.; Ishida, H. *Polymer* **1986**, *27*, 1400.

(34) Wunderlich, B. *Macromolecular Physics*; Academic Press: New York, 1976; Vol. 2.

**Registry No.** PEEK, 31694-16-3; DPE, 101-84-8; DPK, 119-61-9; EEK, 106315-29-1.